Ultrathin Alumina Passivation for Improved Photoelectrochemical Water Oxidation Catalysis of Tin Oxide Sensitized by a Phosphonate-Functionalized Perylene Diimide First Without, and then With, CoO_y

Carly F. Jewell, [†] Ashwanth Subramanian, [#] Chang-Yong Nam, [*, ‡, #] Richard G. Finke[*,†]

[†]Department of Chemistry, Colorado State University, Fort Collins, Colorado, 80523, United States

[‡]Center for Functional Nanomaterials, Brookhaven National Laboratory, Upton, New York, New York 11973, United States

[#]Department of Materials Science and Chemical Engineering, Stony Brook University, Stony Brook, New York 11794, United States

Table of Contents:

S1. Experimental Details for the Atomic Layer Deposition of AlO_x

Ellipsometry Measurement.

To determine the alumina film thickness, the spectral reflectance of Si wafers coated with varying numbers of alumina ALD cycles was measured by a J.A. Woollam M-2000FI ellipsometer. The spectral reflectance data were collected and analyzed using the WVASE32 data acquisition and analysis software (J.A. Woollam Co. Inc.). The incidence angle of the light beam was varied from 50° to 80° with an angle step size of 5°, normal to the substrate plane. The reflectance data were collected over the wavelengths ranging from 200 to 1600 nm. The alumina film thickness was determined by fitting the collected data to a three-layer model (Al_2O_3/native SiO_2/Si) using the known optical constants of the materials available in the software.

Table S1: Results of of alumina measured by ellipsometry as a function of the number of ALD cycles

Number of ALD cycles	Thickness of AlO_x (nm)
2	0.26
5	0.44
10	0.74
15	1.11
20	1.46

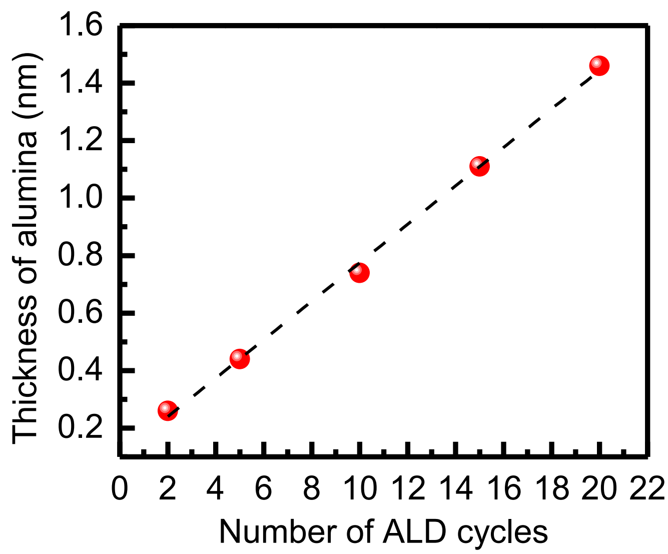

Figure S1: Thickness of alumina measured by ellipsometry as a function of the number of ALD cycles

S2. UV-vis Spectra of Anodes with and without AlO_x

Using a Hewlett Packard 8452A diode array spectrophotometer, UV-vis data were collected on anodes. Anodes were placed directly against the back wall for consistency and a cleaned FTO slide was used as the reference blank.

a.

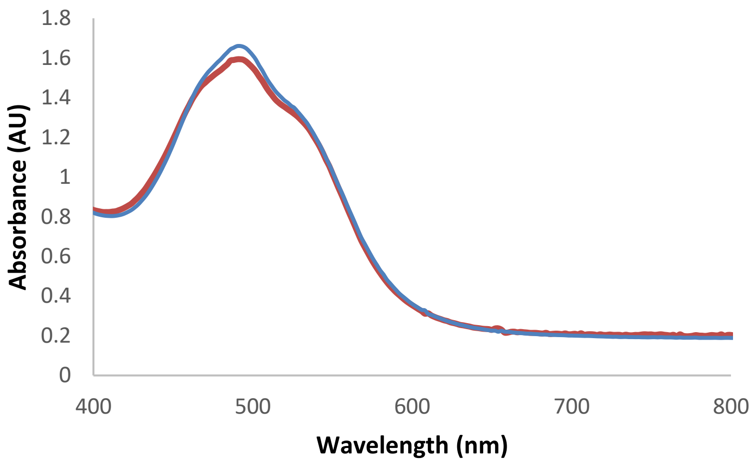

b.

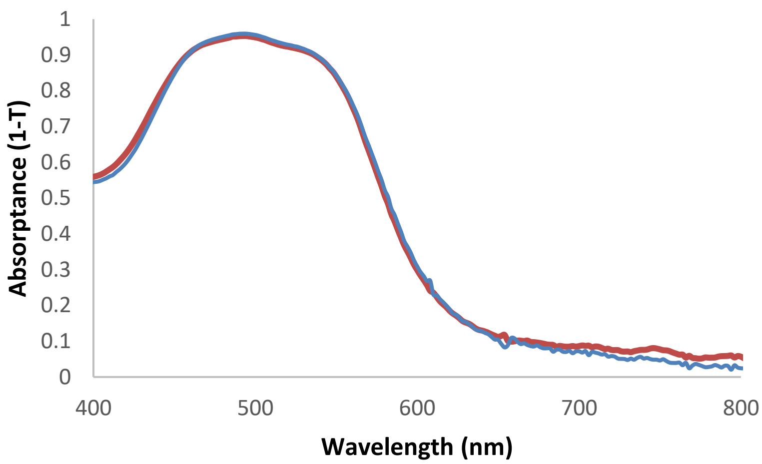

Figure S2: Absorbance (a) and absorptance (b) plot for SnO_2/PMPDI (red) and SnO_2/PMPDI/AlO_x (1.3 nm, 85 °C deposition, blue) anodes. Both the degree to which the dye and SnO_2 absorb light as well as the λ_{max} and absorbance pattern remain unchanged after alumina deposition. The UV-Vis of the anode before and after the ALD indicate the bond between the SnO_2 and the dye was unchanged with the addition of AlO_x at elevated temperatures.

S3. Photocorrosion Controls on SnO_2/PMPDI/AlO_x/CoO_y

Hydroquinone (H_2Q) was added to the system to examine the anode using a more thermodynamically and kinetically facile reaction. An interesting feature of the photocurrent transient data is the spiking behavior. With the addition of H_2Q, a significant decrease in spiking behavior was observed, and the kinetics of the system appear to be shifted in such a way that the recombination in minimized. Our current leading hypothesis for these large spikes at particularly ca. +0.1 V vs Ag/AgCl is photocorrosion, but SnO_2 impurities are certainly another hypothesis. Of note, the conduction band edge for SnO_2 is also in the region of high spiking behavior.[1] This may suggest that there is some photocorrosion occurring due to hole accumulation in the system doing water oxidation, but with the easier oxidation reaction, this can be surmounted.

Another interesting feature seen in photocurrent transient plots is an increased steady-state value at +0.1 to +0.2 V vs Ag/AgCl. We currently have not determined the origin of this feature but favor some combination of photocorrosion, degradation, non-water oxidation faradaic processes, or electrochemical processes relating to the SnO_2. We hypothesize that the defects and impurities in our SnO_2 may be related to this feature. As such, SnO_2 by ALD is of great interest to us and future work will explore this hypothesis.

S4. AlO_x Photoactivity, Disproof of WOCatalyst Character

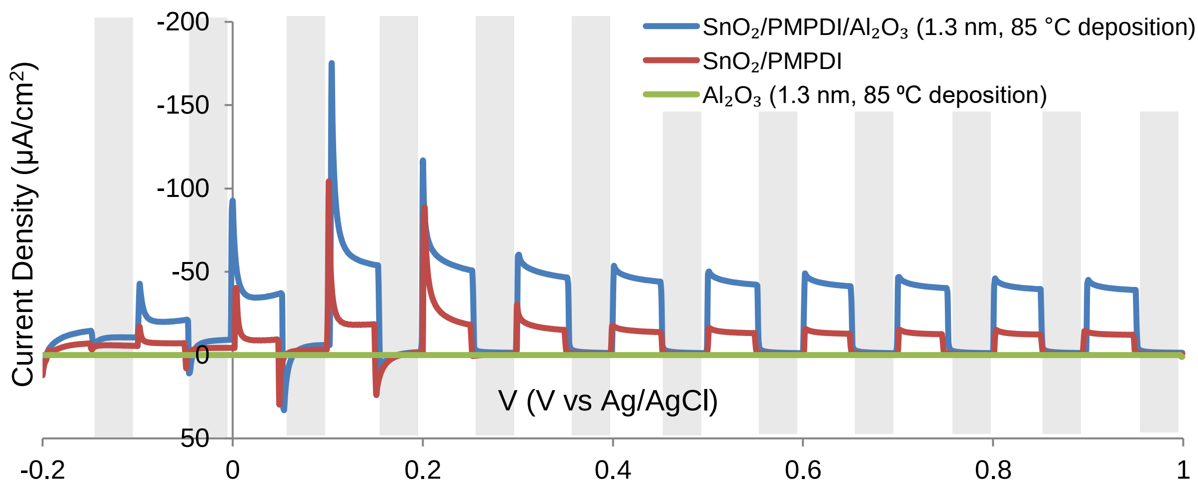

Figure S3: Photocurrent transients (with 5 s light/dark transients indicated by white/ gray shading) for SnO_2/PMPDI/AlO_x anodes (1.3 nm, 85 ºC deposition, blue), SnO_2 /AlO_x (1.3 nm, 85 ºC deposition, red), and AlO_x (1.3 nm, 85 ºC deposition, green). Scans were done from -0.2 to +1.0 V vs Ag/AgCl with 5 second light, then dark transients. Examining the photocurrents, combined with the negligible oxygen production in the latter two cases, indicates that alumina is not functioning as a WOC.

S5. High Resolution XPS of AlO_x

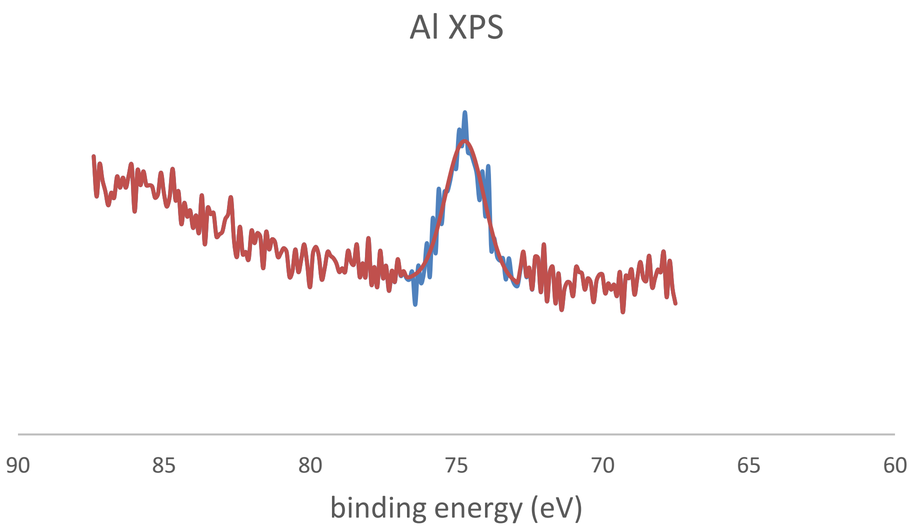

Figure S4: Representative high resolution XPS scan Al 2 p electron on alumina as deposited at 85 °C

XPS was carried out inhouse on a PE-5800 series Multi-Technique ESCA XPS system where a Al Kα monochromatic source operating at 350.0 W was used for all XPS experiments. High resolution (HRES) scans were carried out at a minimum of 3 spots across the sample surface for 30 minutes apiece. To fit the data, CASAXPS software was used to analyze the data. Consistent with both the literature method of XPS fitting and ensuring self-consistency across fits, HRES spectra were calibrated to a 285 eV aliphatic carbon peak.[2,3]

XPS was carried out on a sample of AlO_x deposited at 85 °C. XPS detected only one Al environment, corresponding to the oxide (Figure S4). O deficiencies, which would appear as a peak at a lower binding energy, can certainly impact the conductivity of the alumina layer. However, in all cases one alumina oxide environment was seen and an O deficiency peak is not present.

Of note, cobalt was not visible by XPS even during extended high resolution scans due to the very low, catalytic quantities used.

S6. Thermogravimetric Analysis of PMPDI Stability

To probe the hypothesis that the PMPDI dye was being degraded under the temperatures used for ALD, a control of thermogravimetric analysis of the dye was done. Though the relatively high thermal stability for an organic compound and dye is one of the primary reasons PDI organic dyes are of interest and used in the present work and other devices, this hypothesis was still investigated. TGA was done using a TA Instruments TGA 2950 Thermogravimetric Analyzer under air flow and using a 20 °C/min heating ramp rate (Figure S5). The TGA shows that the dye is stable up to 400 °C, fully consistent with the general literature of PDI dye stability to approximately 300−600 °C.[4]

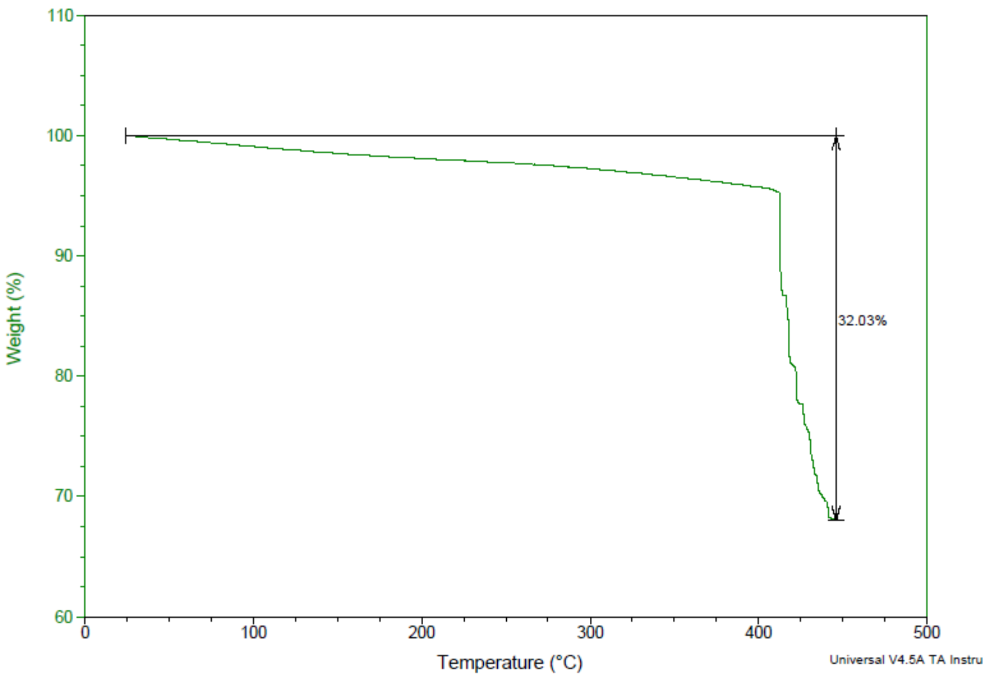

Figure S5. TGA of powder PMPDI from 25-450 °C, ramping 20 °C/minute, and under ambient atmosphere conditions. With increasing temperate, there is minimal weight loss up to 400 °C, indicating PMPDI is stable up to 400 °C. This means all AlO_x depositions herein, ranging from 85 °C to 200 °C, do not cause the PMPDI dye to thermally degrade.

S7. SEM Image of Anodes

Scanning electron microscopy (SEM) images were taken for SnO_2/PMPDI/AlO_x (0.6 nm, 85 °C deposition) anodes to ensure film morphology remained comparable to previously published SEM images of films without alumina.[1] Images were collected using a JEOL JSM-6500F field emission scanning electron microscope (FESEM), using 15 kV accelerating voltage and 10 mm working distance. Porosity in films was observed.

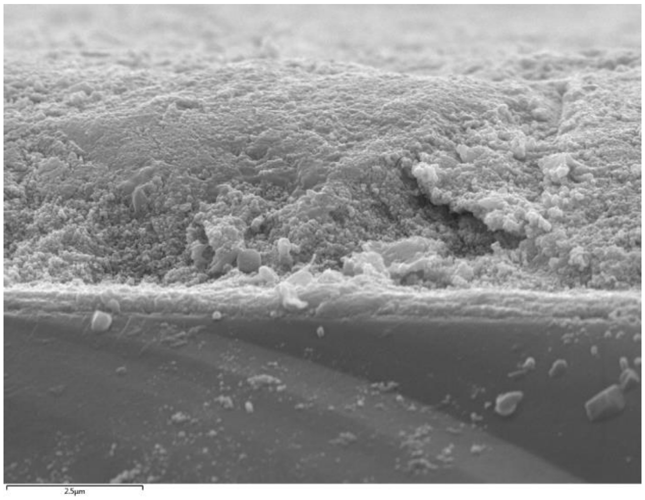

Figure S6: SEM image of SnO_2/PMPDI/AlO_x (0.6 nm, 85 °C)/CoO_y anode taken at 30,000X magnification. Image is a profile of the cross section of the anode after cracking. The FTO glass is clearly visible at the bottom of the SEM image of the cross section for reference and perspective.

SEM-EDS (energy dispersive X-ray spectrometer) data were collected using an Oxford Instruments energy dispersive X-ray spectrometer and Oxford Aztec software was used for qualitative and quantitative elemental analysis. A SnO_2/PMPDI/AlO_x (0.6 nm, 85 °C)/CoO_y anode was cracked in half in order to examine the cross section (Figure S6). The anode was then coated in 10 nm of gold. The cross section of the anode was then examined using SEM-EDS, though the sample had to be oriented at a slight angle off of vertical, in order to determine if cobalt was seen throughout the sample. Cobalt was not detected due to the very low, catalytic quantity used.

S8. Photocurrent Measurement for Optimized Anode for Decay:

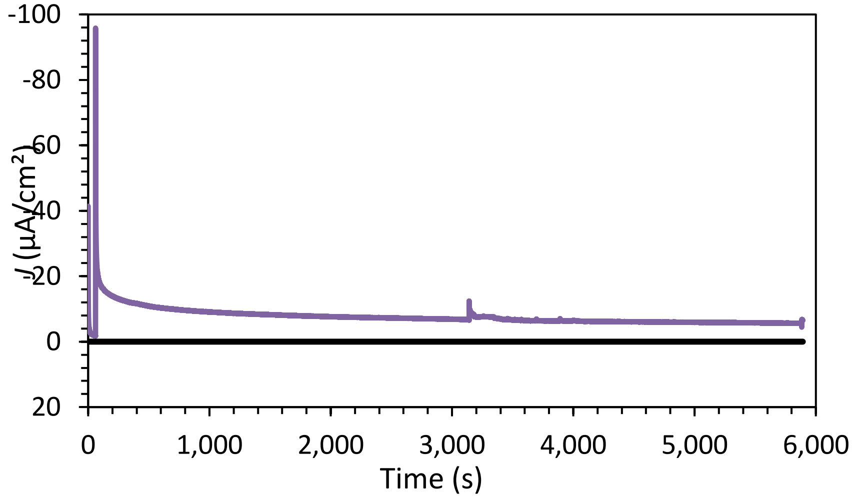

Figure S7: i-t of a representative SnO_2/PMPDI/AlO_x/CoO_y (0.6 nm, 85 °C deposition) anode performed at +0.2 V vs Ag/AgCl in pH 7, 0.1 M KPi buffer. Measurements were taken for over 90 minutes to look at photocurrent decay.

In order to understand the longevity of the photoanode system, the photocurrent of a representative SnO_2/PMPDI/AlO_x (0.6 nm, 85 °C deposition)/CoO_y anode was measured at +0.2 V vs Ag/AgCl. In an extended, ca. 1.5 hour long, experiment, a significant, 78%, decay in photocurrent generation was noted. Replicate O_2 detection experiments displayed a decay of O_2 evolution by 11% after four replicate trials (1200 s).

S9. Experimental Details for SnO_2/AlO_x/PMPDI System

Deposition of AlO_x was also done on the nano-SnO_2 rather than the SnO_2/PMPDI in order to determine if a more optimal placement of the layer could be achieved. Previously, attempts were made to deposit Al_2O_3 by a solution-based methodology[1], but the observed photocurrents were decreased compared to the system without alumina. Increased dye loading was observed with the addition of the alumina layer in that prior study, although any benefit of increasing the tunneling barrier was counteracted by a reduced injection yield.[1]

Herein, once again we observed significantly increased dye deposition kinetics on the SnO_2/AlO_x system. However, the dye deposited onto the SnO_2/AlO_x anodes using the same elevated temperature dying technique discussed in the main text proved extremely unstable physically; any slight movement or agitation in water immediately resulted in the dye flaking off of the anode. Attempts were made to dye the anodes from room temperature solution over a longer period as well as at elevated temperature for a shorter period; however, in every instance the dye immediately fell off the anodes once removed from solution.

In future studies, the use of a less aggregated[5–9] derivative of the dye could potentially help reduce this preferential binding and stacking of the dye with itself rather than with the SnO_2/AlO_x.

References:

(1) Kirner, J. T.; Finke, R. G. Sensitization of Nanocrystalline Metal Oxides with a Phosphonate- Functionalized Perylene Diimide for Photoelectrochemical Water Oxidation with a CoO_x Catalyst. *ACS Appl. Mater. Interfaces* **2017**, *9*, 27625–27637.

(2) Evans, S. Correction for the Effects of Adventitious Carbon Overlayers in Quantitative XPS Analysis. *Surf. Interface Anal.* **1997**, *25*, 924–930.

(3) Greczynski, G.; Hultman, L. X-Ray Photoelectron Spectroscopy: Towards Reliable Binding Energy Referencing. *Progress in Materials Science*. Elsevier Ltd January 1, 2020, p 100591.

(4) Pasaogullari, N.; Icil, H.; Demuth, M. Symmetrical and Unsymmetrical Perylene Diimides: Their Synthesis, Photophysical and Electrochemical Properties. *Dye. Pigment.* **2006**, *69*, 118–127.

(5) Hagfeldt, A.; Boschloo, G.; Sun, L.; Kloo, L.; Pettersson, H. Dye-Sensitized Solar Cells. *Chem. Rev.* **2010**, *110*, 6595–6663.

(6) Mishra, A.; Fischer, M. K. R.; Büuerle, P. Metal-Free Organic Dyes for Dye-Sensitized Solar Cells: From Structure: Property Relationships to Design Rules. *Angew. Chemie - Int. Ed.* **2009**, *48*, 2474–2499.

(7) Lindquist, R. J.; Phelan, B. T.; Reynal, A.; Margulies, E. A.; Shoer, L. E.; Durrant, J. R.; Wasielewski, M. R. Strongly Oxidizing Perylene-3,4-Dicarboximides for Use in Water Oxidation Photoelectrochemical Cells. *J. Mater. Chem. A* **2016**, *4*, 2880–2893.

(8) Chen, Z.; Stepanenko, V.; Dehm, V.; Prins, P.; Siebbeles, L. D. A.; Seibt, J.; Marquetand, P.; Engel, V.; Würthner, F. Photoluminescence and Conductivity of Self-Assembled Pi-Pi Stacks of Perylene Bisimide Dyes. *Chem. - A Eur. J.* **2007**, *13*, 436–449.

(9) Gallaher, J. K.; Aitken, E. J.; Keyzers, R. A.; Hodgkiss, J. M. Controlled Aggregation of Peptide-Substituted Perylene-Bisimides. *Chem. Commun.* **2012**, *48*, 7961–7963.